Astron. Astrophys. 299, 596–610 (1995)

ASTRONOMY
AND
ASTROPHYSICS

Empirical models of solar magnetic elements: constraints imposed by Mg I Stokes profiles

C. Briand[1] **and S.K. Solanki**[2]

[1] Centre Universitaire d'Orsay, I.A.S, Bât 121, F-91405 Orsay CEDEX, France
[2] Institut für Astronomie, ETH-Zentrum, CH-8092 Zürich, Switzerland

February 7, 1995

Abstract. Although the temperature structure of small-scale magnetic features in the lower and middle photosphere has been constrained quite well, there are still considerable uncertainties in the upper photospheric and lower chromospheric thermal structure. As a step towards an improvement of this situation we investigate, using a non-LTE analysis, the diagnostic capabilities of the Stokes I and V profiles of the Mg I b_2 517.3nm and the Mg I 457.1nm lines. We find that the V profile of the former line can constrain the magnetic element thermal and velocity structure near the temperature minimum, which goes beyond the capabilities of the commonly used Fe I and II lines. The λ457.1nm line, on the other hand, does not provide any additional information on its own. A comparison of synthetic profiles with plage and network Stokes I and V spectra confirms the findings of Bruls & Solanki (1993) that the chromospheric temperature rise starts at a substantially lower height in magnetic elements than in the quiet Sun. Some of the ambiguities in previous empirical models of magnetic elements are also removed. We confirm that small-scale magnetic features are associated with larger line broadening velocities than the quiet Sun, particularly in the higher layers. Finally, the Mg I b_2 line is revealed to be a direct diagnostic of the merging height of magnetic elements.

Key words: Sun: magnetic fields – Sun: activity – Sun: faculae

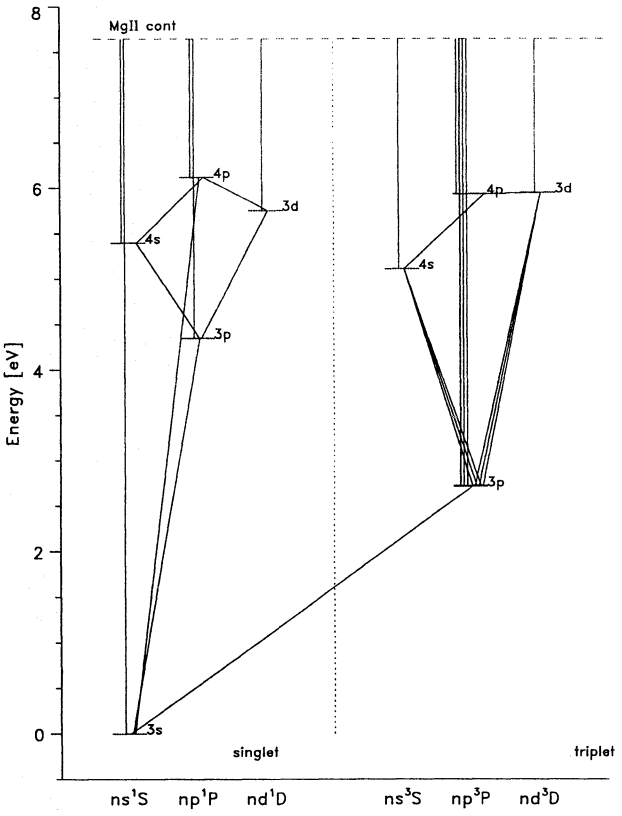

Fig. 1. Term diagram of the atomic model used in the computations

1. Introduction

There is increasing evidence that the lower solar chromosphere is highly structured, with hot flux tubes embedded in a medium that is at least in part cooler than the minimum temperature of traditional solar atmospheric models (e.g. Ayres & Testerman 1981; Ayres 1981; Ayres et al. 1986; Solanki & Steiner 1990; Solanki et al. 1991, 1994). The cool non-magnetic parts of the lower chromosphere can be studied using CO vibration-rotation transitions in the infrared (Ayres et al. 1986; Uitenbroek et al. 1994). Comparable diagnostics for the upper photosphere and lower chromosphere of small-scale intense magnetic features (referred to here as magnetic elements) are not so well developed. A knowledge of the upper photospheric or chromospheric temperature structure is important, however, to constrain heating mechanisms. Initial constraints on the onset of the temperature rise in magnetic elements were set by Bruls & Solanki (1993, hereafter BS93). They found that the chromospheric temperature rise starts at deeper layers within magnetic elements in plage and network regions than in the quiet Sun, mainly from the Stokes V profile shape of Fe II 492.3nm. A chromospheric

Table 1. Adopted atomic parameters of the investigated transitions. The first column gives the wavelength of the transitions considered, the second identifies the levels involved. Their energies are indicated in the third column. The fourth column lists the oscillator strength, the fifth column the radiative damping and the last column the effective Landé factor

wavelength (nm)	Label	E (cm^{-1})	f	G_a (s^{-1})	g_{eff}
457.11	3s3p ^3P to 3s^2 ^1S	21870.464 to 0.000	3.55×10^{-6}	4.30×10^{2}	1.50
517.27	3s4s ^3S to 3s3p ^3P	41197.403 to 21870.464	1.37×10^{-1}	1.02×10^{8}	1.75

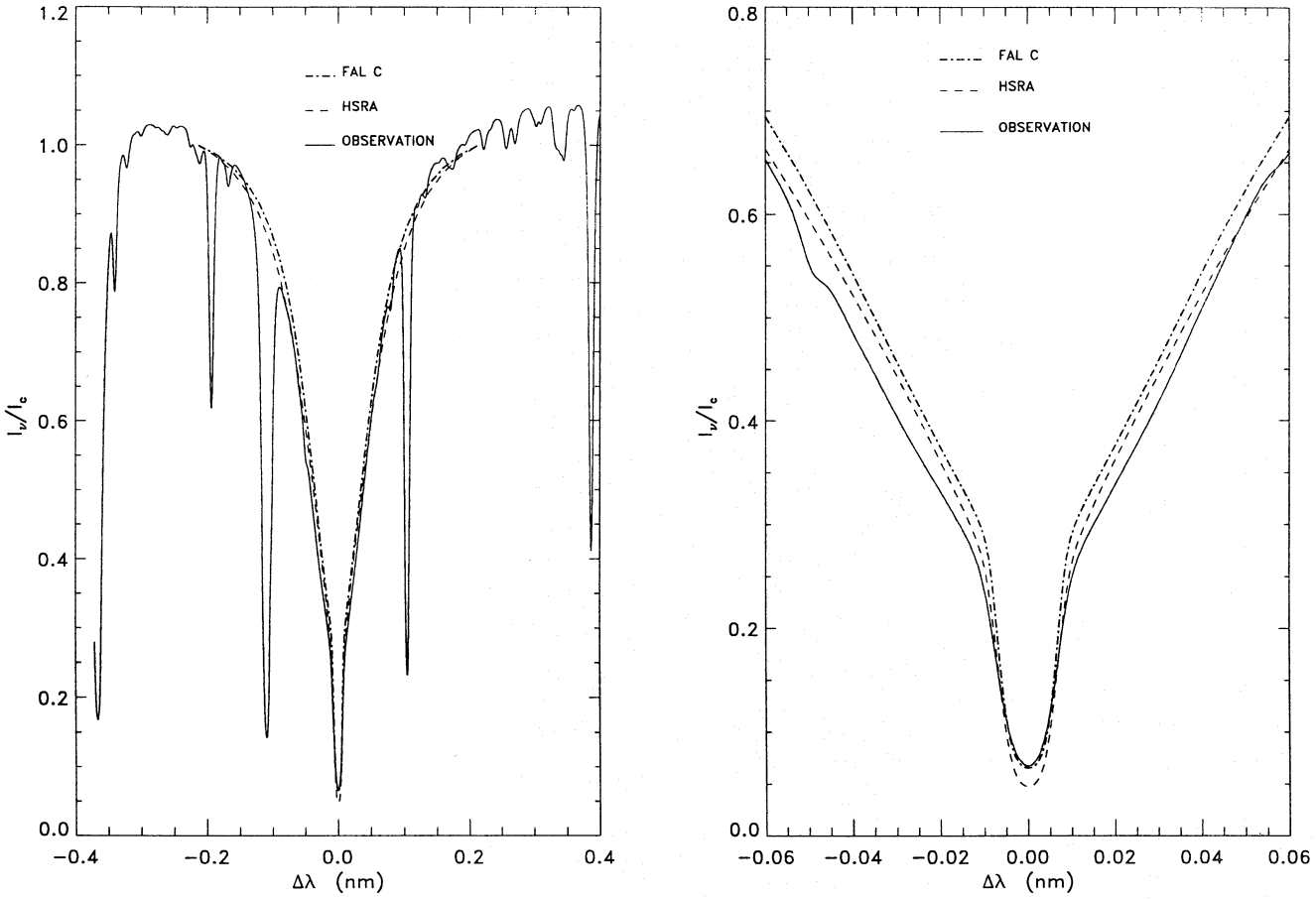

Fig. 2. Comparison of the Mg I b_2 line profiles computed using HSRA and FAL C with an observed quiet Sun profile. The right panel shows a close-up of the central part of the line

onset in deeper layers creates an inversion in the core of the V profile of this line, since it is formed close to Local Thermodynamic Equilibrium (LTE). However, the Fe I and II lines they used are not sufficiently temperature sensitive to unambiguously determine the actual height of the start of this temperature enhancement or the temperature structure of the layers immediatly below it. Lites et al. (1987) studied sunspot umbrae using observations of the Mg I intercombination line at λ457.1nm, which, at least in umbrae, shows a similar behaviour to Fe II 492.3nm in hotter atmospheres. They concluded from the observed V profile shape that the chromospheric temperature rise starts higher than in the umbral atmosphere of Maltby et al. (1986). Another approach was taken by Solanki et al. (1991). They constrained the temperature above the level of the traditional temperature minimum using observations of the unpolarized Ca II K line core. Since the non-magnetic atmosphere also contributes significantly to the unpolarized profile, this approach has its limitations. Polarized observations, such as those of Martínez Pillet et al. (1990) may extend the capabilities of the Ca II K line to diagnose magnetic element thermal structure. Finally, Walton (1987) employed the wings of the Mg I b_2 line to constrain the temperature in his facular model.

We take yet another approach which combines elements of the approaches described above. We simulate Stokes I and V profiles of λ457.1nm and the stronger b_2 λ517.3nm line and compare these with profiles observed in an active region plage and in enhanced network. Both lines are calculated in non-LTE (NLTE), although for the former this is an unnecessary precaution. By using Stokes V we ensure that we achieve considerably more unique results, since Stokes V is sensitive mainly to the

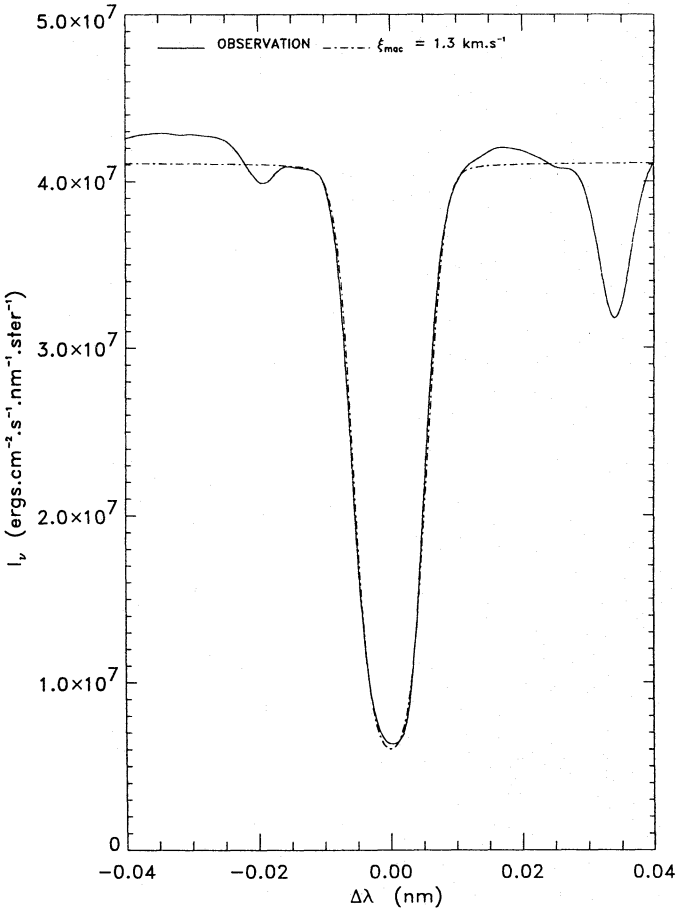

Fig. 3. Comparison of the observed and computed profiles of the 457.1nm line in the quiet Sun. The microturbulence is 1 km s^{-1}, the macroturbulence is 1.3 km s^{-1}

atmosphere within the magnetic elements. Its use thus allows us to overcome some of the observational problems associated with the small horizontal size of magnetic elements.

We are also interested in the line broadening velocity in the upper photopheric layers of magnetic elements relative to the quiet Sun values. Any enhancement within the magnetic elements would be suggestive of an enhanced wave flux, which might be related to the deeper chromosphere within magnetic elements. Early work suggested a total turbulent velocity within magnetic elements that is considerably larger than in the quiet Sun (Solanki 1986). More recent and considerably refined estimates (e.g. based on NLTE studies) show a smaller difference (BS93). These estimates are based on weak or medium strength iron lines whose flanks get their main contributions from the lower or mid photosphere. Here we consider the much stronger b_2 line, whose core should give us information on the broadening velocity in the upper photosphere.

The observed Stokes I and V spectra with which the computed profiles are compared have been obtained with the FTS polarimeter at the McMath-Pierce telescope on Kitt Peak on 29-30 April 1979. The data have high spectral resolution and S/N ratios, but low spatial resolution. For more details on the observations see Stenflo et al. (1984) and Solanki (1987). We have three spectra of the λ517.3 nm line at our disposal. They were obtained in the enhanced network and a strong plage (Stokes I and V), and in the quiet Sun (Stokes I only). For the λ457.1nm line we possess I and V spectra from strong plage and the network. The spectrum of this line in the quiet Sun is taken from the Kitt Peak atlas (White et al. 1972). All the observations were carried out near the center of the solar disk (μ = 0.92 for the plage, μ = 0.98 for the network, and $\mu \approx 1$ for the quiet Sun).

In Sects. 2, 3 and 4 we outline the computational method, atomic model and atmospheres used. In Sect. 5 we investigate whether these lines have the necessary diagnostic capabilities. Finally, we present the results in Sect. 6 and discuss them in Sect. 7.

2. Computational methods

The NLTE computations of Stokes profiles are based on the field-free approximation (Rees 1969), i.e. on the assumption that the Zeeman splitting does not alter the populations of the levels. We expect that this approximation is valid since the line is formed sufficiently deep in the atmosphere for the Zeeman sublevels to be collisionally coupled together (Auer et al. 1977). Thus, the radiative transfer equation may first be solved using a code that does not treat polarization effects in order to obtain level populations and opacities. A second code then formally solves the transfer equation for the Zeeman split Stokes vector using the source function, level populations, Doppler width, damping constant and opacities obtained in the first step.

We use a revised version of MULTI (Scharmer & Carlsson 1985; Carlsson 1986) to compute the first step, i.e. to carry out unpolarized radiative transfer in a plane parallel medium, with NLTE line source functions. The version we use can treat each transition with complete or partial redistribution in frequency (Uitenbroek 1989). However, the Mg I b_2 and the intercombination line are formed sufficiently deep in the atmosphere to enable us to neglect partial redistribution effects. For the second step, namely the calculation of the Stokes parameters, we employ the code SPSR developed by Rees et al. (1989) and Murphy & Rees (1990) which computes the Stokes profiles by solving the Unno-Rachkovsky equations. It is based on the DELO (Diagonal Element Lambda Operator) method.

3. Atomic model

We employ a Mg I atomic model consisting of 11 levels plus a continuum, with 15 transitions. Tests with different atomic models show that this model reproduces the lines of interest to sufficient accuracy at a minimum cost of computing time. The atomic scheme is given in Fig. 1. Table 1 lists some of the adopted values of parameters describing the two transitions investigated here.

All the parameters adopted are the ones used by Carlsson et al. (1992) for the computation of the 12μm Mg I lines, except for the treatment of the triplet 3p ^3P. In order to properly compute

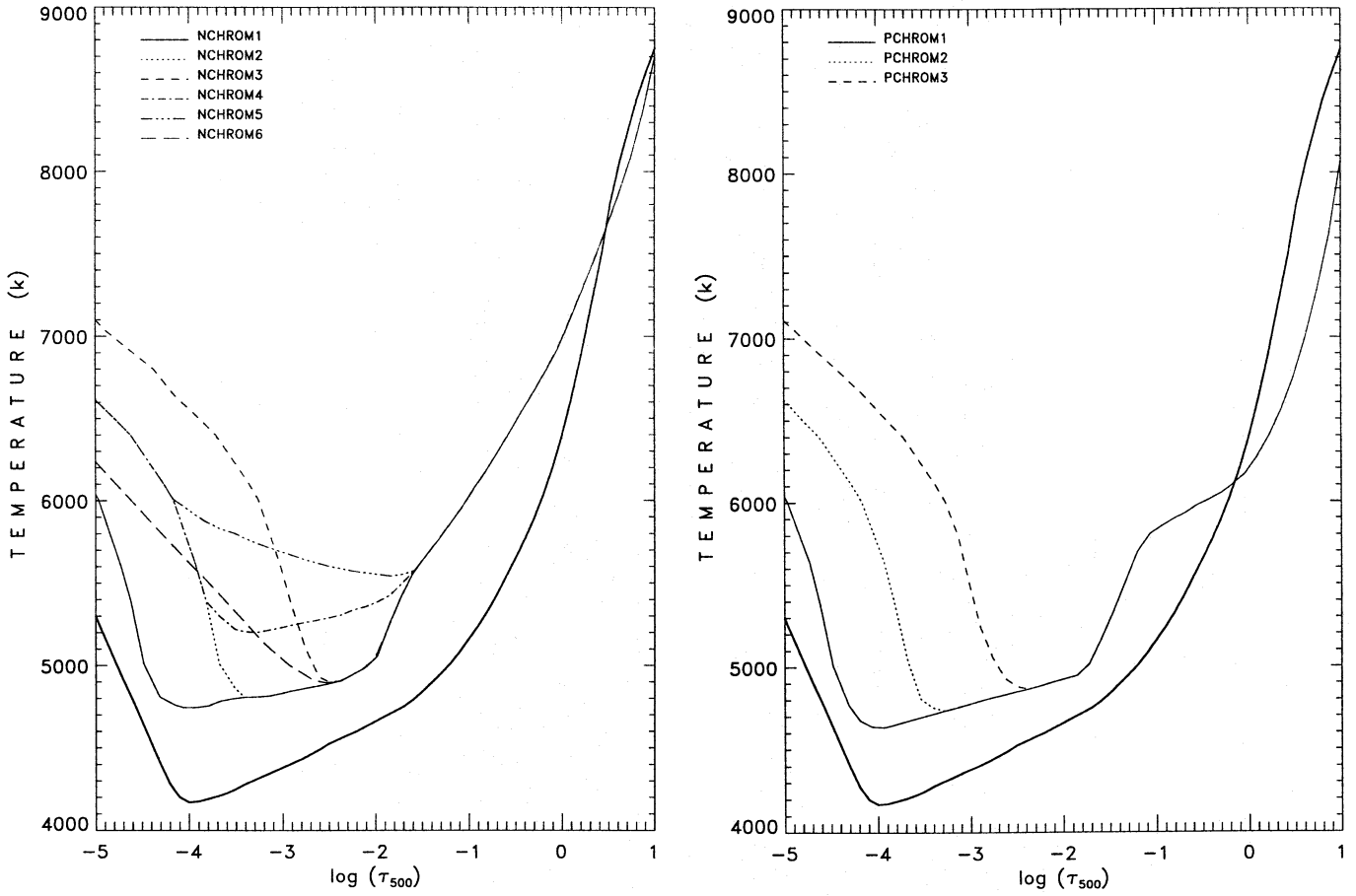

Fig. 4. Temperature T versus logarithmic continuum optical depth at 500nm, $\log(\tau_{500})$, of atmospheric models of network (left frame) and plage (right frame) magnetic elements (models taken from BS93). In both plots the thick line represents the HSRA (quiet Sun)

the λ457.1nm and λ517.3nm lines, we consider the three levels of this triplet separately.

The f values have been taken from Mendoza & Zeippen (1987), except for the transition between $3s^2\ ^1S_0$ and $3s3p\ ^3P_1$ for which f has been chosen such as to provide a good fit of observations of the quiet Sun. The radiative parameters are calculated following Unsöld (1955). The λ517.27nm line is very sensitive to the amount of van der Waals damping. According to Lwin et al. (1977) and O'Neil & Smith (1980) van der Waals broadening may be better reproduced by a $T^{0.4}$ dependence rather than the traditional $T^{0.3}$ one. We have tested the two dependences, employing the formula given by Unsöld (1955) for the $T^{0.3}$ dependence and modifying it according to the recipe provided by O'Neil & Smith (1980) for the $T^{0.4}$ dependence:

$$\Gamma_6 = g_6 \alpha n_H T^n,$$

where n_H is the hydrogen number density, T is the temperature, $n = 0.3$ or 0.4, and g_6 is the Van der Waals parameter. In accordance with previous investigators we have allowed the g_6 obtained from the Unsöld formula to be enhanced by a multiplicative factor α. If we allow this factor to be a free parameter then we can obtain almost identical profiles for both temperature dependences. We have adopted the $T^{0.3}$ dependence, with a g_6 factor of 1 and 5 for the λ457.1nm and λ517.3nm lines, respectively.

Photoionisation has been explicitly computed for all levels. The values come from Hofsaess (1979). We have checked that the resonance peaks in the photoionisation cross-sections do not influence the profile of the lines under study.

Collisional rates for bound-free transitions were calculated with Seaton's approximation, as given by Allen (1976)

4. Atmospheric models

4.1. General structure of the model

The model we consider for the atmospheric structure is composed of two components: a magnetic component described by a flux tube, embedded in a non-magnetic medium which is described by a model of the quiet Sun. The magnetic and pressure stratification of the flux tube component is based on the thin tube approximation (e.g. Defouw 1976; Schüssler 1986), i.e. horizontal and vertical force balance is decoupled, and reduced to strict pressure balance:

$$P_i(z) + \frac{B^2(z)}{8\pi} = P_e(z)$$

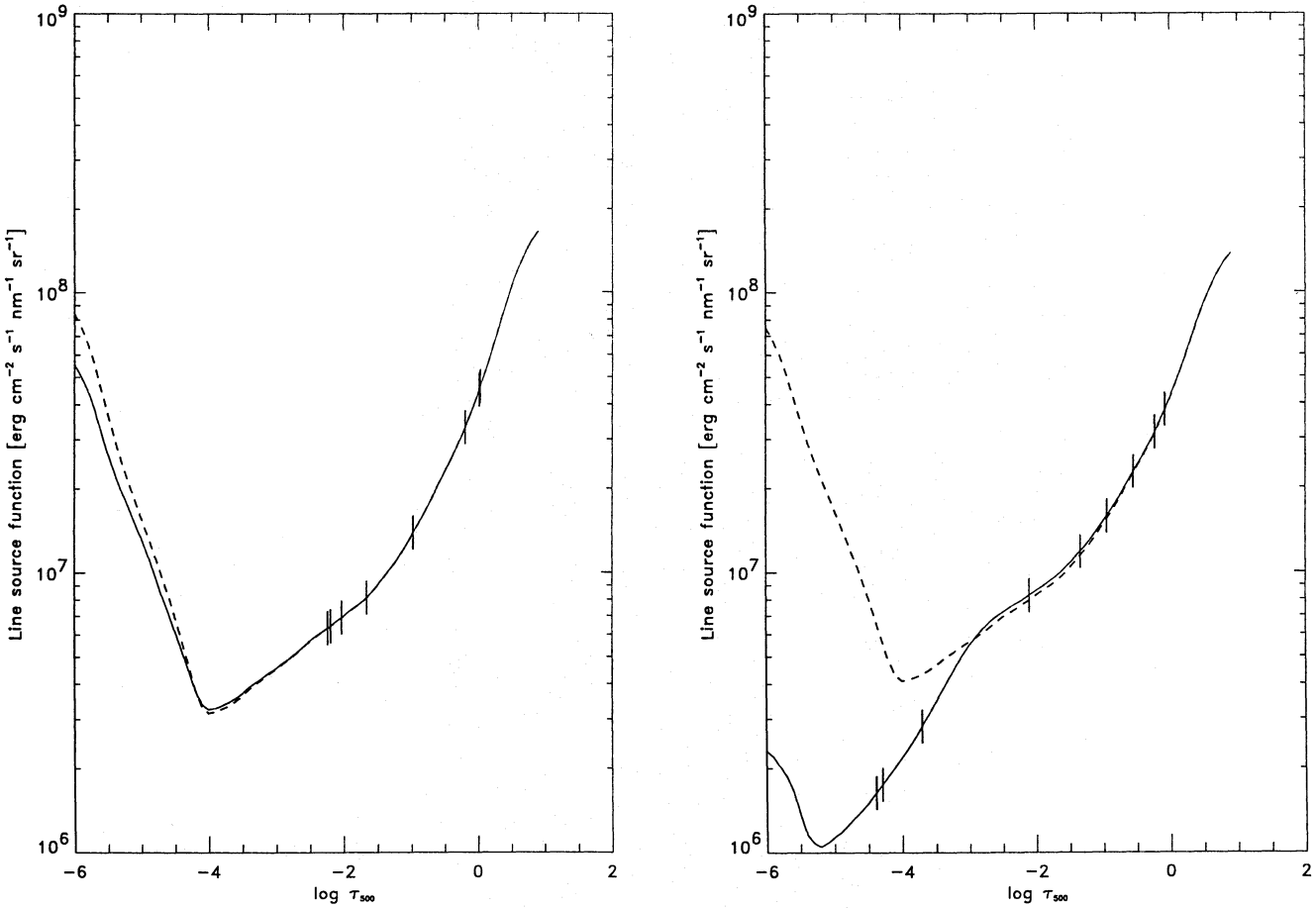

Fig. 5. Line source functions (solid) compared to the Planck function (dashed) at different wavelengths in the line for the quiet Sun (HSRA). Left frame: λ457.1nm; right frame: λ517.3nm. The vertical ticks indicate the location of τ_ν=1 at different wavelengths in each line (from left to right $\Delta\nu$ = 0., 0.8, 1.7, 3.0, 4.5, 6.4, 9.2, 13.1, 18.8 and 27.3pm for λ457.1nm and 0., 1.7, 4.0, 7.5, 13.8, 25.4, 48.4, 94.7pm and 0.189nm for λ517.3nm)

$$\frac{dP}{dz} = -\rho g_\odot$$

The first equation describes the horizontal pressure equilibrium. $P_i(z)$ and $P_e(z)$ are the height dependent gas pressures in the interior and exterior of the flux tube, respectively, and B is the magnetic field strength. The second equation describes hydrostatic equilibrium, with ρ being the gas density and $g_\odot$ the solar gravitational acceleration. Turbulent pressure is neglected, in accordance with the finding that turbulent velocities derived from the fits to the Mg I lines are clearly subsonic. In order to completely describe the flux tubes, conservation of magnetic flux is imposed and the equation of state is prescribed. Instead of employing an energy equation we determine the thermal structure from a fit to the observations.

Since the external gas pressure decreases with height the flux tube expands, until it merges with its neighbours. This merging height depends on the filling factor α, i.e. on the fractional area covered by magnetic structures at the level at which τ_{500}=1 in the quiet Sun (e.g. Spruit & Roberts 1983; Pneuman et al. 1986).

The radiative transfer is carried out along 10 rays parallel to the axis of symmetry of the flux tube. Their distance from the flux tube axis is chosen such that the intersection points of the various rays with the flux tube boundary are equally spaced in the vertical direction (cf. Solanki & Roberts 1992). Consequently, each ray represents a plane-parallel atmosphere, composed in general of a magnetic (upper) and a non-magnetic (lower) part. Stokes I and V profiles are computed along each ray independently, i.e. lateral radiative transfer is neglected. The weighted average of all computed profiles is then compared with the observations. The weighting takes into account the cylindrical geometry of the flux tube and the inequal horizontal spacing of the rays.

4.2. Non-magnetic atmospheres (quiet Sun)

Figure 2 shows a comparison between Stokes I profiles of λ517.3nm computed with two quiet Sun models (HSRA, Gingerich et al. 1971; and FAL C, Fontenla et al. 1993) and observations obtained in the quiet Sun. The microturbulence, ξ_{mic}, is 1 km s^{-1} and no macroturbulence has been employed for these calculations. Although the core of the computed profile is too deep, the flanks and inner wings are better reproduced by the

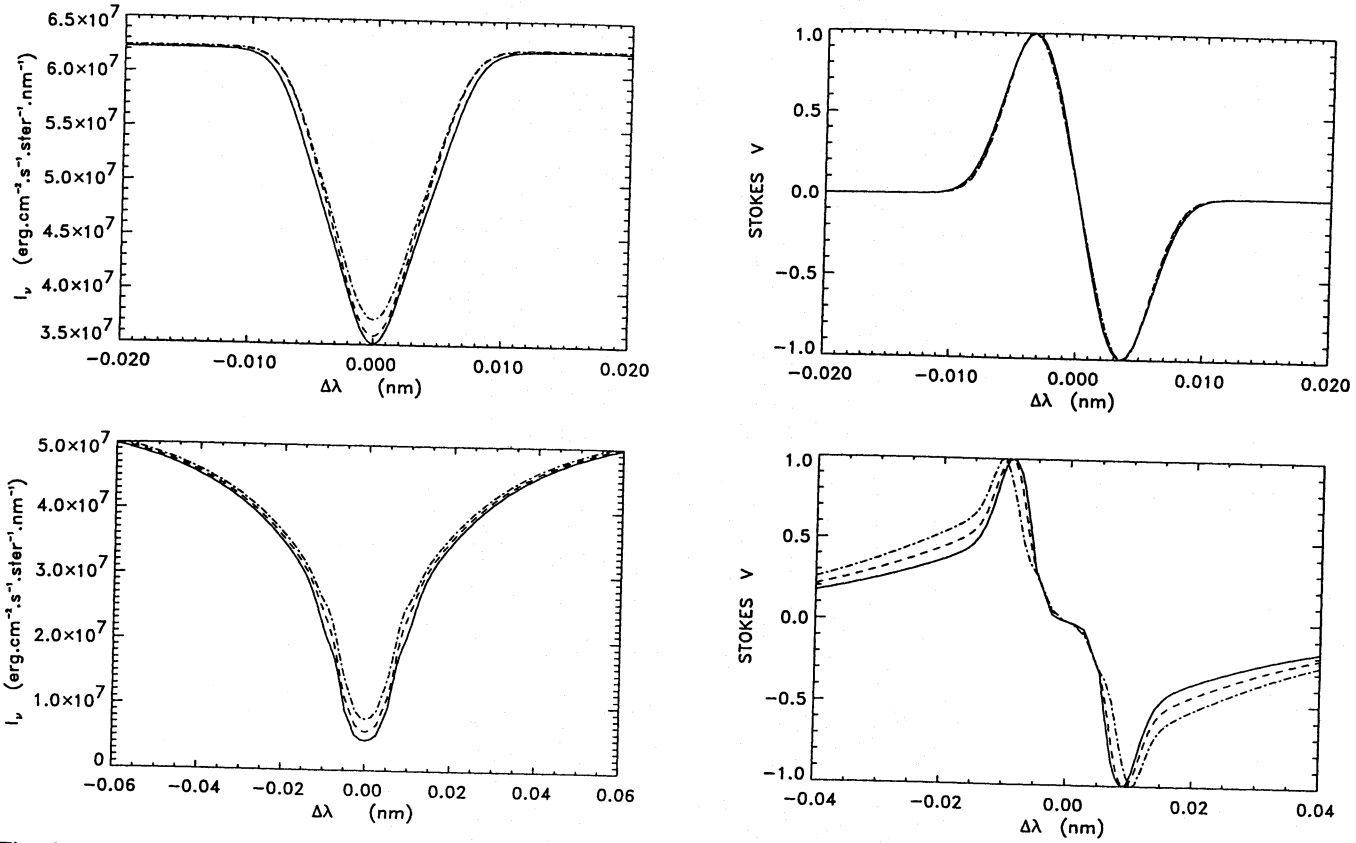

Fig. 6. Stokes I and V profiles of λ457.1nm (upper panels) and λ517.3nm (lower panels) synthesized for different network models: — NCHROM2, – – NCHROM4, · – NCHROM5. The V profiles have been normalized to unit amplitude to highlight differences in profile shape

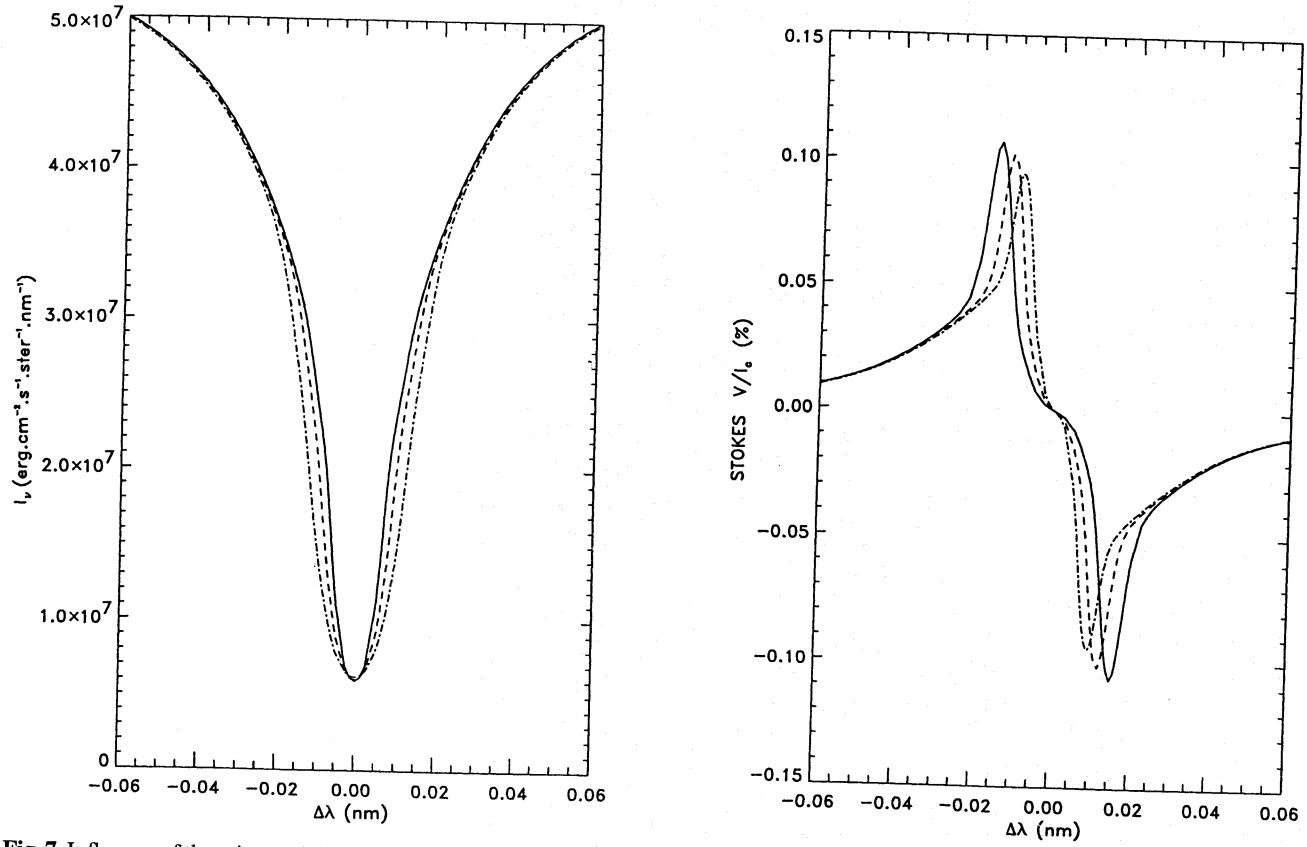

Fig. 7. Influence of the microturbulent velocity ξ_{mic} on the Stokes I and V profiles of λ517.3nm computed for the NCHROM4 model atmosphere. —: 1 km s^{-1}; – –: 2 km s^{-1}; – · –:3 km s^{-1}

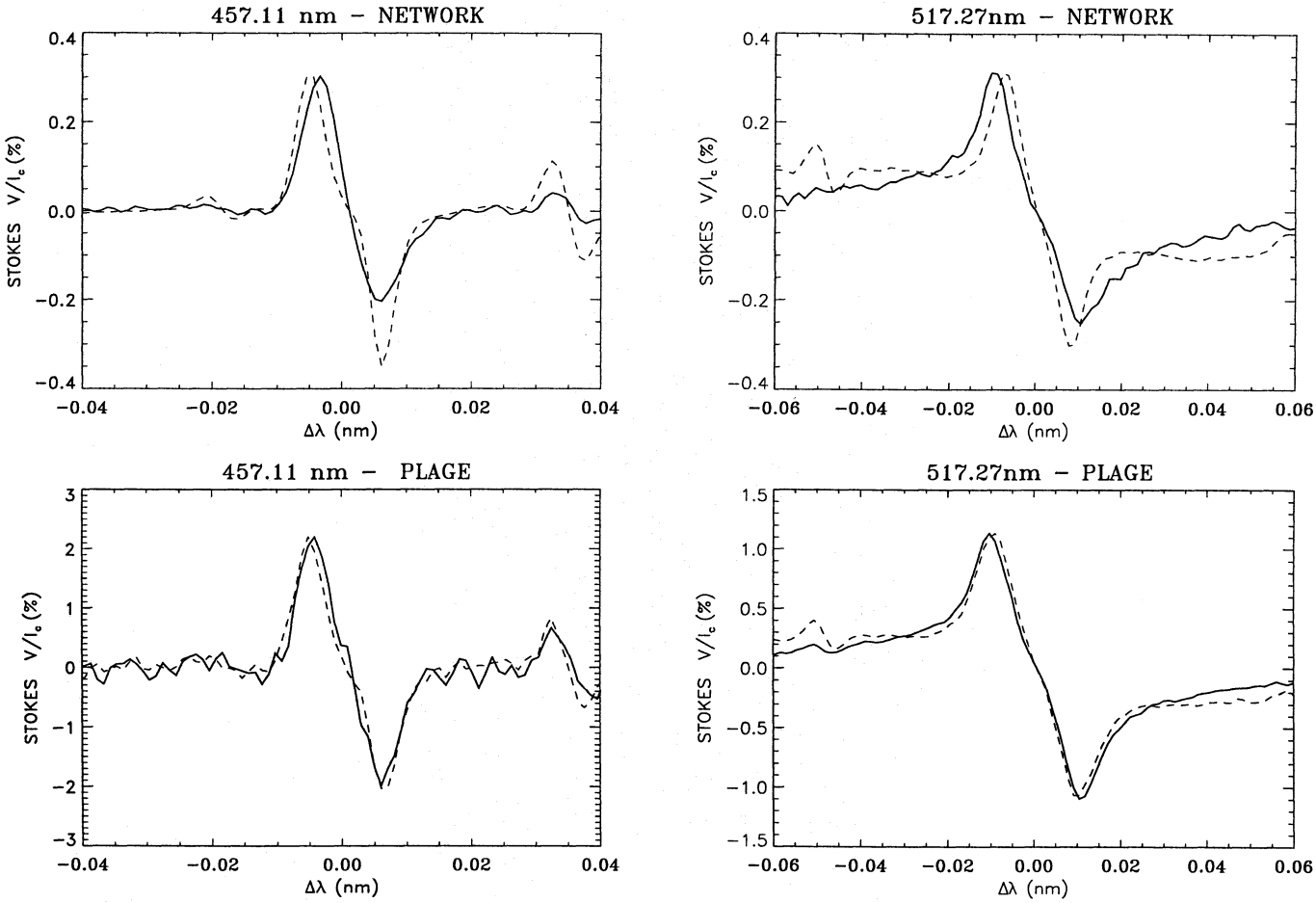

Fig. 8. Comparison of Stokes V (solid) with $\frac{dI}{d\lambda}$ (dashed) as observed in the network (upper panels) and in an active region plage (lower panels). The intercombination line is plotted on the left, the b_2 line on the right

HSRA. Since these parts of the line have the best diagnostic capabilities for our purposes (see Sect. 5), we have adopted the HSRA as the non-magnetic component for all our models. The Holweger & Müller (1974) model provides an even better fit to the observed profile of this line (Lemke 1986), but the absence of a chromospheric temperature rise takes it out of contention for the present purposes.

Figure 3 illustrates the result of a computation of the intercombination line with the HSRA. A macroturbulent velocity must be employed for a typical photospheric line such as this. We have found that the best result is obtained for a value of 1.3 km s^{-1}. The remaining difference between observed and computed profile is due to the asymmetry of the line which is not of consequence for the present analysis.

4.3. Magnetic atmospheres

The magnetic elements in the network and in plage regions have different temperature structures (e.g. Hirayama 1978; Solanki & Stenflo 1984). Thus, Solanki (1986) and Keller et al. (1990) constructed different atmospheres for network and plage flux tubes. Grossmann-Doerth et al. (1994) have demonstrated that the lower temperature of magnetic features in regions with large filling factor (plage) relative to features in regions with smaller filling (network) can be explained by the existence of slightly larger flux tubes in the former case. The thermal structures appear to differ mainly in the lower photospheric layers. In particular, the chromospheric temperature rise does not appear to depend too strongly on the filling factor (BS93). We start our investigation with the only set of Stokes V based empirical models that includes a chromospheric temperature rise, namely the nine models constructed by BS93. The thermal profiles of these models are plotted in Fig. 4 (cf. also BS93).

Line profile calculations based on these models (Sect. 5) show that the Mg I b_2 line is a better diagnostic of upper photospheric temperature than the Fe II 492.3nm, the line used most heavily by BS93. Thus, although their observations were accurately reproduced by more than one of their models, we find that the b_2 line observations are not satisfied by any of them. Therefore, after an initial set of calculations with the BS93 models we construct further models that are modifications of the best fit BS93 models. Basically, we first modify the $T(\tau)$ stratification and then calculate the rest of the atmospheric parameters consistently therefrom. We then compute the Mg I lines in this modified model, compare them with the observations and iterate until the latter are reproduced to our satisfaction.

5. Sensitivity of the lines to atmospheric parameters

The Mg I lines in the optical are not particularly sensitive to the magnetic field strength and should always be used in conjunction with a magnetic diagnostic such as the 525.02/524.71

Stokes V line ratio. Fortunately, the FTS spectra analysed here include these two Fe I lines, and the field strengths for the observed plage and network regions are well known (e.g. Solanki et al. 1987; Keller et al. 1990). In the following we therefore only need to investigate the capabilities of the two Mg I lines to diagnose temperature and turbulence velocity.

5.1. Temperature

The λ457.1nm line is a forbidden transition. Consequently, variations of electron density will influence the rate of the transition. This line is thus formed very close to LTE, as may be seen from Fig. 5. This finding is in good agreement with previous results (e.g. Lemke 1986; Mauas et al. 1988). The λ517.3nm line is formed over a greater height range and its core is formed at a height at which the source function has decoupled from the Planck function. However, except in its core, this line is still formed very close to LTE. Consequently both lines are expected to be temperature sensitive.

In order to quantify these findings and to observe the influence of temperature changes on Stokes I and V, we have computed the profiles for all the atmospheres constructed by BS93. Only a single ray corresponding to the flux tube axis is considered for these initial test calculations. The most informative comparison is between models NCHROM2, NCHROM4 and NCHROM5. These atmospheres differ mainly in the mid and upper photosphere (Fig. 4). The resulting Stokes I and V profiles of the two lines are plotted in Fig. 6. The V profile shape of the λ517.3nm line is much more sensitive to temperature variations than the λ457.1nm Stokes V. The lack of sensitivity of the V profile *shape* of λ457.1nm to temperature is disappointing. This line is too strongly weakened in all three models to react to the chromospheric temperature like Fe II 492.3nm, i.e. by showing an inversion in its core, particularly in Stokes V. The shape of this line does react, however, if the temperature is lowered, e.g. to below the quiet Sun value. [1]

The dominant effect of the temperature rise in the upper half of the photosphere on the λ517.3nm V profile is to broaden and move the peaks apart and to strengthen the inner wings. This is basically a consequence of the weakening of this line in response to increasing temperature. In the weakened Stokes I profile the core extends to greater intensities, i.e. to greater λ (corresponding to outwards shifted Stokes V peaks) and the wings are weaker, i.e. steeper (leading to stronger Stokes V wings). Recall that in a homogeneously magnetized atmosphere, such as the ones used for these calculations, $V \sim \frac{dI}{d\lambda}$ for a weakly split line. This condition is fulfilled to a high degree by both Mg I lines, even in the presence of a kilogauss field. It is important to note that the λ517.3nm V profile shape can distinguish between models 2 and 4, although both are equally consistent with Fe I and II polarimetric data (BS93).

The I profiles of both line are almost equally sensitive to temperature, as can be seen from the left-hand panels of Fig. 6.

[1] The V amplitude of this line changes from model to model, but this property is shared with, e.g., most of the iron lines and does not deserve closer scrutiny at present.

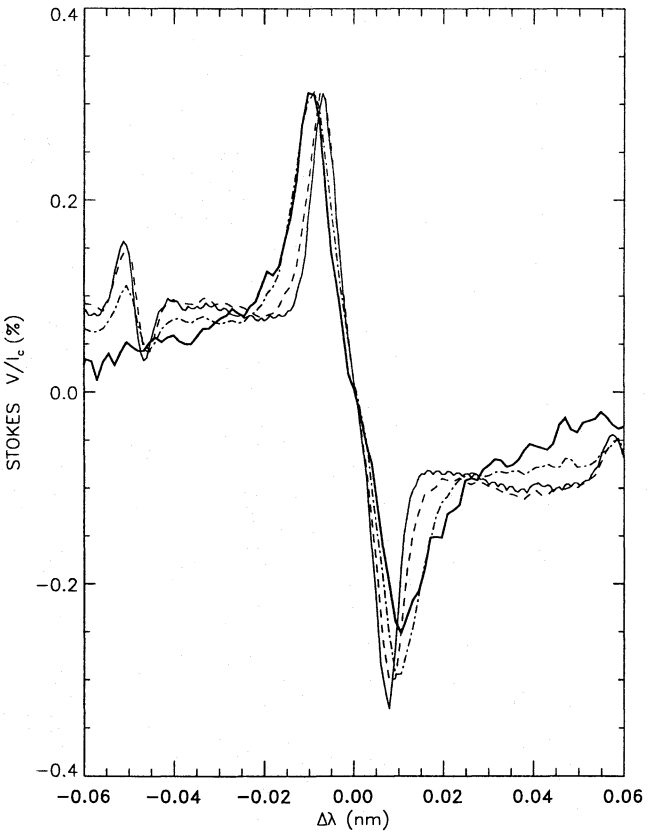

Fig. 9. Stokes I and V profiles of the λ517.3nm line computed with NCHROM2(– –), NCHROM4 (·–) and NCHROM6 (solid line) compared to the observations (thick solid curve)

However, as a consequence of the greater sensitivity of its Stokes V profile shape, we shall use λ517.3nm as the main diagnostic and the intercombination line only to check the results.

5.2. Microturbulence

Microturbulence, ξ_{mic}, produces a broadening of the Stokes I profile of λ517.3nm (Fig. 7, left hand panel) and influences the shape of the V profile (Fig. 7, right hand panel). The maxima of the Stokes V σ-components move apart as ξ_{mic} increases, but their width is not modified. The core becomes flatter, while the wings remain unaffected. Again, the behaviour of V is simply a reflection of the broadening of Stokes I via $V \sim \frac{dI}{d\lambda}$. The main point to note is that the I and in particular the V profile are affected in a different manner by ξ_{mic} than by the temperature (this is true also for the other temperature stratifications tested). For example, the V profile shows no enhancement of the wings with increasing ξ_{mic}.

6. Results

6.1. Observed V and $\frac{dI}{d\lambda}$ profiles

Consider first the observed profiles. The observed Stokes V (solid) and $\frac{dI}{d\lambda}$ (dashed) profiles are plotted in Fig. 8 for the network (upper panel) and plage (lower panels).

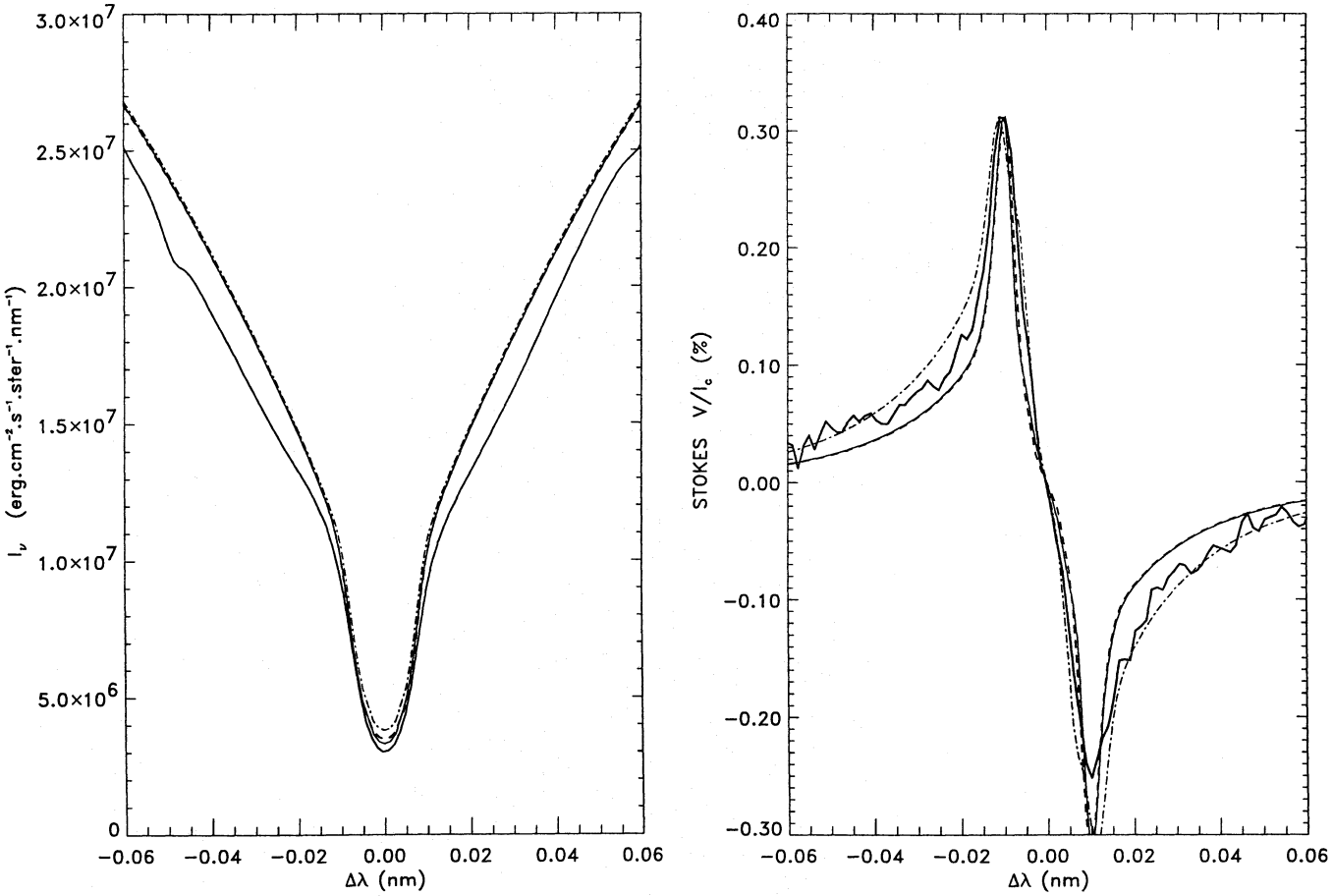

Fig. 10. Stokes V profile (thick solid line) of λ517.3nm observed in a network, as well as $\frac{dI}{d\lambda}$ obtained in the quiet Sun (—), network (– –) and plage (– · –)

Most apparent is the similarity between $\frac{dI}{d\lambda}$ and V in the plage and the difference between them in the network. The difference is not due to the breakdown of the weak-field approximation; the two lines are simply too broad and Zeeman insensitive for that. Rather, it points to differences in the atmospheres in which Stokes I and V are formed. In the network, which has a small magnetic filling factor, Stokes I gets hardly any contribution from inside the magnetic features and almost only samples the non-magnetic fraction of the atmosphere. In the plage, on the other hand, Stokes I also gets a non negligible contribution from the magnetic elements. Note that except for the asymmetry, the Stokes V profiles from the two solar regions have very similar shape, it is mainly the I profile which changes. To illustrate this we plot in Fig. 9 $\frac{dI}{d\lambda}$ of λ517.3nm in the quiet Sun, network and plage, together with its network V profile. Note how $\frac{dI}{d\lambda}$ approaches Stokes V in shape as the magnetic filling factor increases.

A more subtle point is also visible in Figs. 8 and 9. The plage V and $\frac{dI}{d\lambda}$ profiles of λ517.3nm agree relatively well in the line core, but differ by increasingly larger amounts in the line wings with increasing distance from the core. A similar behaviour is also exhibited by the wings of the network profile. We propose the following qualitative explanation for this observation. In the lower photosphere the magnetic filling factor is relatively small, so that the differences between the two components of the atmosphere manifest themselves as differences between $\frac{dI}{d\lambda}$ and V in the wings of λ517.3nm (due to the larger filling factor in the plage, this effect is smaller there). At greater height the flux tubes have expanded so that I and V sample more nearly the same atmosphere. Consequently V and $\frac{dI}{d\lambda}$ are more similar to each other in the inner wings. In the plage the flux tubes are sufficiently close to each other to merge at approximately the formation height of the λ517.3nm core, i.e. in the temperature minimum layer, while in the network the merging takes place in a higher layer (e.g. Pneuman et al. 1986; Steiner & Pizzo 1989; Solanki & Steiner 1990). Thus V and $\frac{dI}{d\lambda}$ are similar in the core of the plage profile, but different in the core of the network profile. The asymmetry of the network V profile is likely of the same origin as the asymmetry of photospheric V profiles, i.e. due to light passing into the magnetic elements from the downflows surrounding them (Grossmann-Doerth et al. 1988). In the following we make no attempt to model the asymmetry

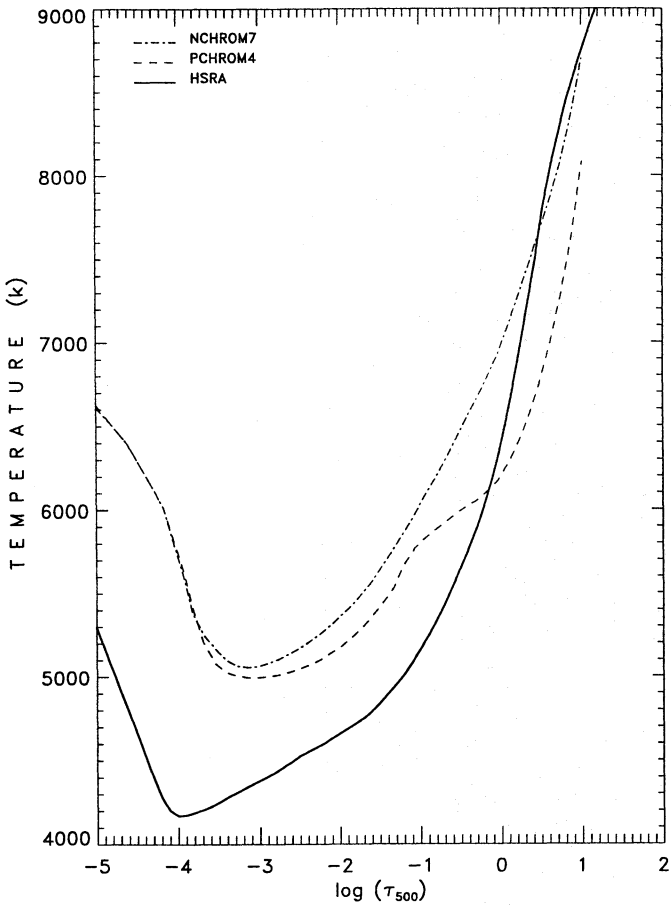

Fig. 11. Temperature T vs. logaritmic continuum optical depth $\log(\tau_{500})$ of the new atmosphere for network magnetic elements NCHROM7, plage magnetic elements PCHROM4, and the quiet Sun model HSRA (solid line). The flux tube temperature is largely unconstrained by observations for $\log \tau_{500} \leq -4$

and mainly try to reproduce the blue wings of the observed profiles.

The observed profiles on their own thus already suggest that the λ517.3nm line is not only a good diagnostic of the thermal structure, but actually responds to the flux tube expansion and magnetic merging height, making it a unique diagnostic in this respect. In the following we describe the more quantitative results of the modelling.

6.2. Network

As pointed out by BS93, the models NCHROM2, NCHROM4 and NCHROM6 reproduce the Stokes V profiles of Fe I and II lines almost equally well. Consequently, we have first compared the line profiles resulting from these particular models with the observations (Fig. 10). Those can distinguish between these three models if we concentrate mainly on Stokes V. In accordance with previous analyses of this FTS spectrum, a filling factor of 5% combined with 1.5-D radiative transfer along 10 rays and $B(z = 0) = 1500$G are used and turn out to be satisfactory values of these parameters. The non-magnetic component is described by the HSRA with height independent microturbulence fixed at 1 km s^{-1}. The magnetic component also has a height independent microturbulence derived by fitting the observations, which gives 1.6 km s^{-1} within an error of $\pm$0.1 km s^{-1}. None of the models provides a perfect fit to Stokes V, with NCHROM4 coming closest to this aim. The fits to Stokes I also all leave something to be desired (interestingly the quiet Sun HSRA model reproduces the plage I profile very well).

Figure 10 suggests that the fit could be improved by adopting a temperature structure lying betweeen NCHROM2, which is too cool, and NCHROM4, which is too hot. After a few iterations, we obtained a reasonable fit to the Mg I lines (except for the V asymmetry) with a new atmosphere, which we name NCHROM7, whose temperature stratification is shown in Fig. 11 (dot-dashed curve).

The best fits to the I and V profiles of both lines are shown in Figs. 12 and 13. We have given greater weight to the Stokes V profile when carrying out the fits to derive the new model.

6.3. Plage

We modelled the plage observations in a similar manner to the network data (Sect. 6.2). To demonstrate the necessity of creating a new model to describe plage magnetic elements we plot in Fig. 14 the I and V profiles of the b_2 line resulting from the PCHROM2 model, which BS93 found to adequately reproduce observed iron lines. A microturbulence of 1 km s^{-1}, a value compatible with the iron line data, was chosen (no macroturbulence was used, however).

The maximum of the computed V profile is too close to line center, indicating a too small value of the microturbulence. Moreover, the σ components are too narrow and the line wings are too weak. Although an increased microturbulent velocity can shift the σ-peaks to the correct wavelength, it affects neither their width nor the strength of the wings (cf. Sect. 5.2). To improve the correspondence with the observations in these respects as well, it is necessary to increase the temperature in the upper photosphere. The temperature of the plage flux tube model finally adopted after a number of trials, PCHROM4, is plotted in Fig. 11 (dashed curve). The microturbulent velocity of the best fit is 1.8 $\pm$ 0.1 km s^{-1}. The I and V profiles of the two lines resulting from PCHROM4 are plotted in Figs. 15 and 16, respectively, together with the observed profiles.

7. Discussion and conclusion

In the present paper, we have investigated the response of the Stokes I and V profiles to the turbulent velocity and to the temperature in the upper photosphere and lower chromosphere. We have, in a second step, used the newly developed diagnostics to improve empirical models of the thermal structure of magnetic elements. The Mg I b_2 line proves to be a sensitive diagnostic

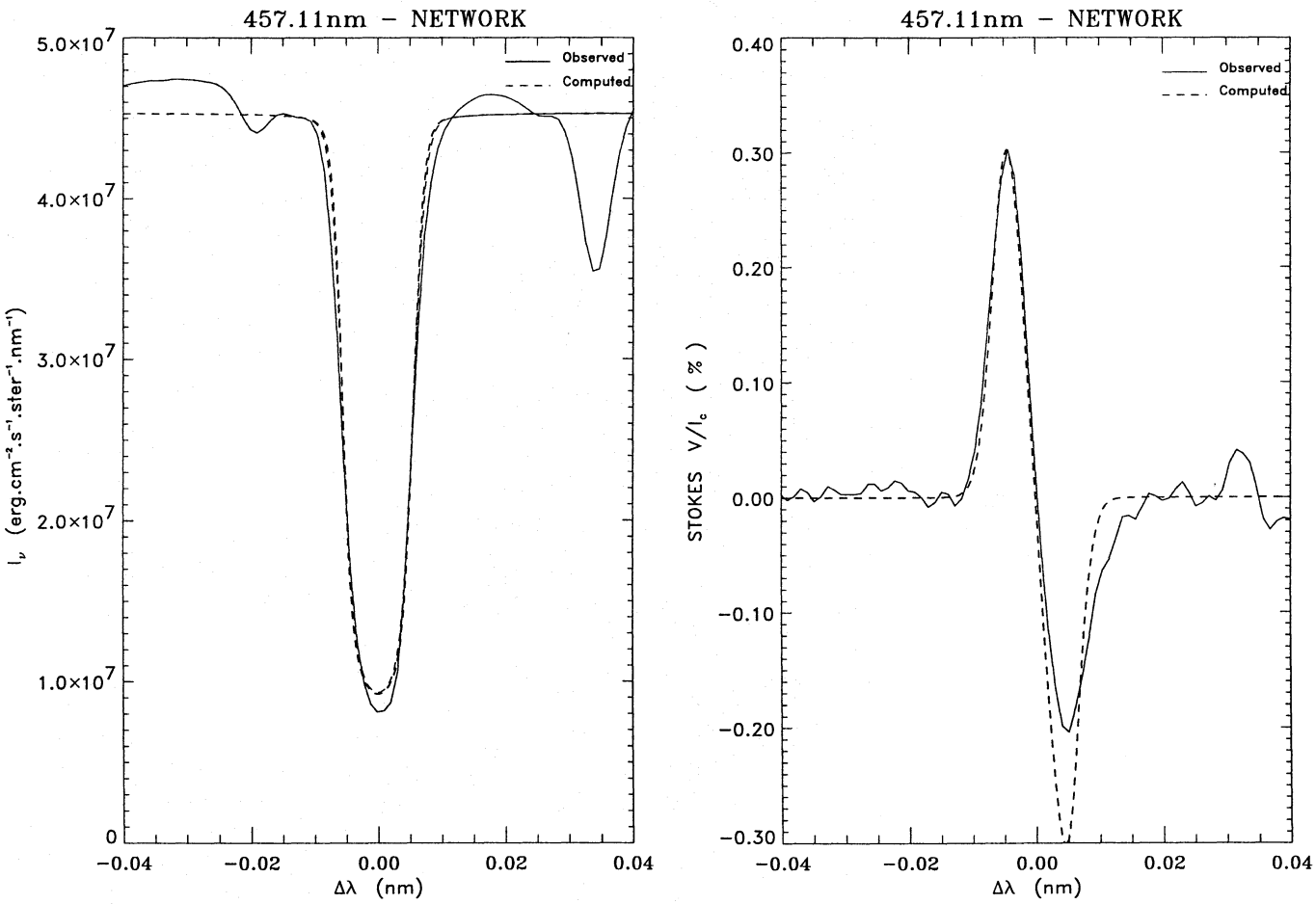

Fig. 12. Stokes I and V profiles for the λ457.1nm line observed in the network and resulting from the NCHROM7 atmosphere (1.5-D radiative transfer)

of the temperature minimum level in magnetic elements. In particular, the shape of the V profile shows a different response to changes in temperature and microturbulence, making it a powerful tool for obtaining these parameters independently. This line is more sensitive to temperature in the upper photosphere than the Fe I and II lines used by BS93. It can thus distinguish between models that reproduce the iron line data equally well. In addition, the b_2 line is formed over a sufficiently large height range to actually respond to flux tube expansion with height (Sect. 6.1). It thus bridges a sensitive gap in the diagnostics available previously. It is, however, necessary to carry out the analysis in NLTE to make full use of the potential of this line. The 457.1nm intercombination line, on the other hand, can be calculated in LTE, but is not particularly useful on its own in constraining the temperature (in sunspots the situation changes and the line can become an important diagnostic, as pointed out by Lites et al. 1987).

Our detailed fits to observations suggest that although magnetic elements in plages and in the network have, on average, different temperature structures, as suggested by previous analyses (Solanki & Stenflo 1984; Solanki 1986; Keller et al. 1990; Solanki & Brigljević 1992), this difference is restricted to the lower photosphere. In the upper photosphere and the lower chromosphere the thermal structures of the magnetic features appear to converge, in agreement with earlier conclusions drawn by Solanki et al. (1991), and BS93. Grossmann-Doerth et al. (1994) could explain the temperature difference in the lower photosphere simply by postulating that magnetic elements in active region plage (with large magnetic filling factor) are on average slightly larger than the average magnetic element in the network (small magnetic filling factor) and we propose that the difference in thermal structure in the lower photosphere is due almost entirely to the difference in radiative flow into magnetic elements in the network and the plages. The similarity of the chromospheric temperature rises in the two regions, on the other hand, suggest that the transport and deposition of energy in the upper photosphere and lower chromosphere does not depend strongly on the size of the magnetic element (within limits; pores and sunspots must have a lower energy deposition rate). This naturally explains the decreasing difference between $T(\tau)$ of the two models with increasing height. In both models, the chromospheric rise of the temperature starts at about $\log(\tau_{500}) \approx -3.5$,

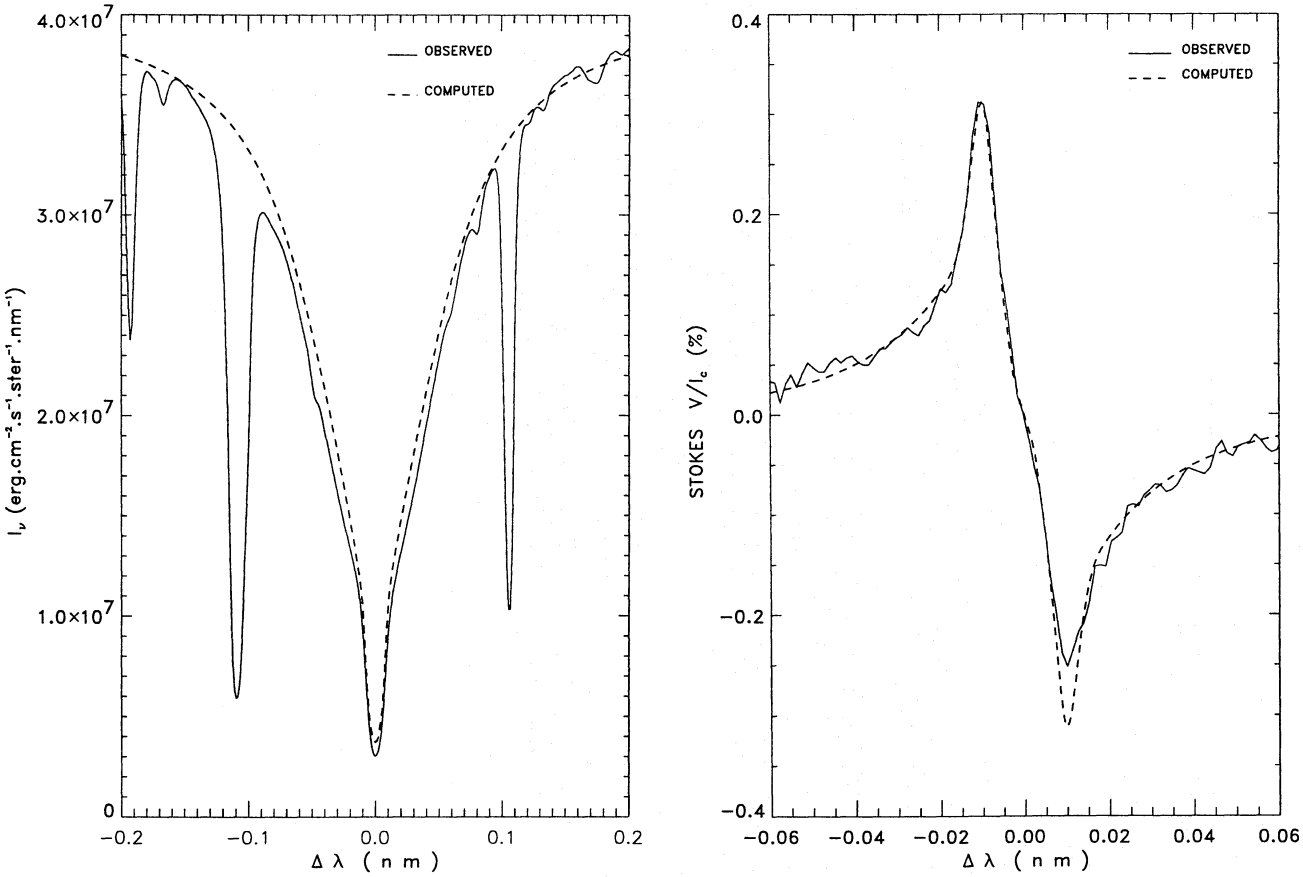

Fig. 13. The same as Fig. 12 for the λ517.3nm line

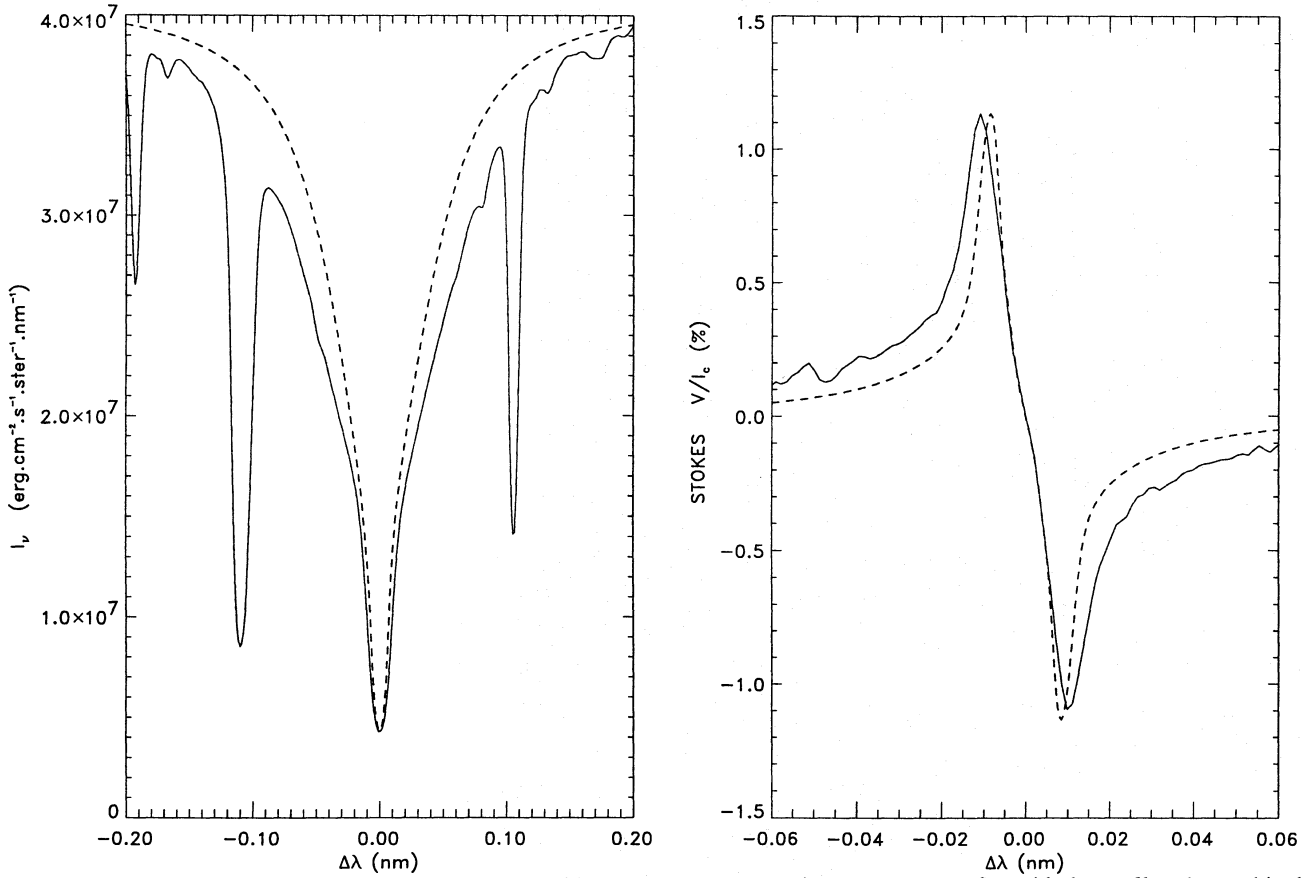

Fig. 14. Stokes I and V profiles of the b_2 line computed with PCHROM2 as magnetic component together with the profiles observed in the plage

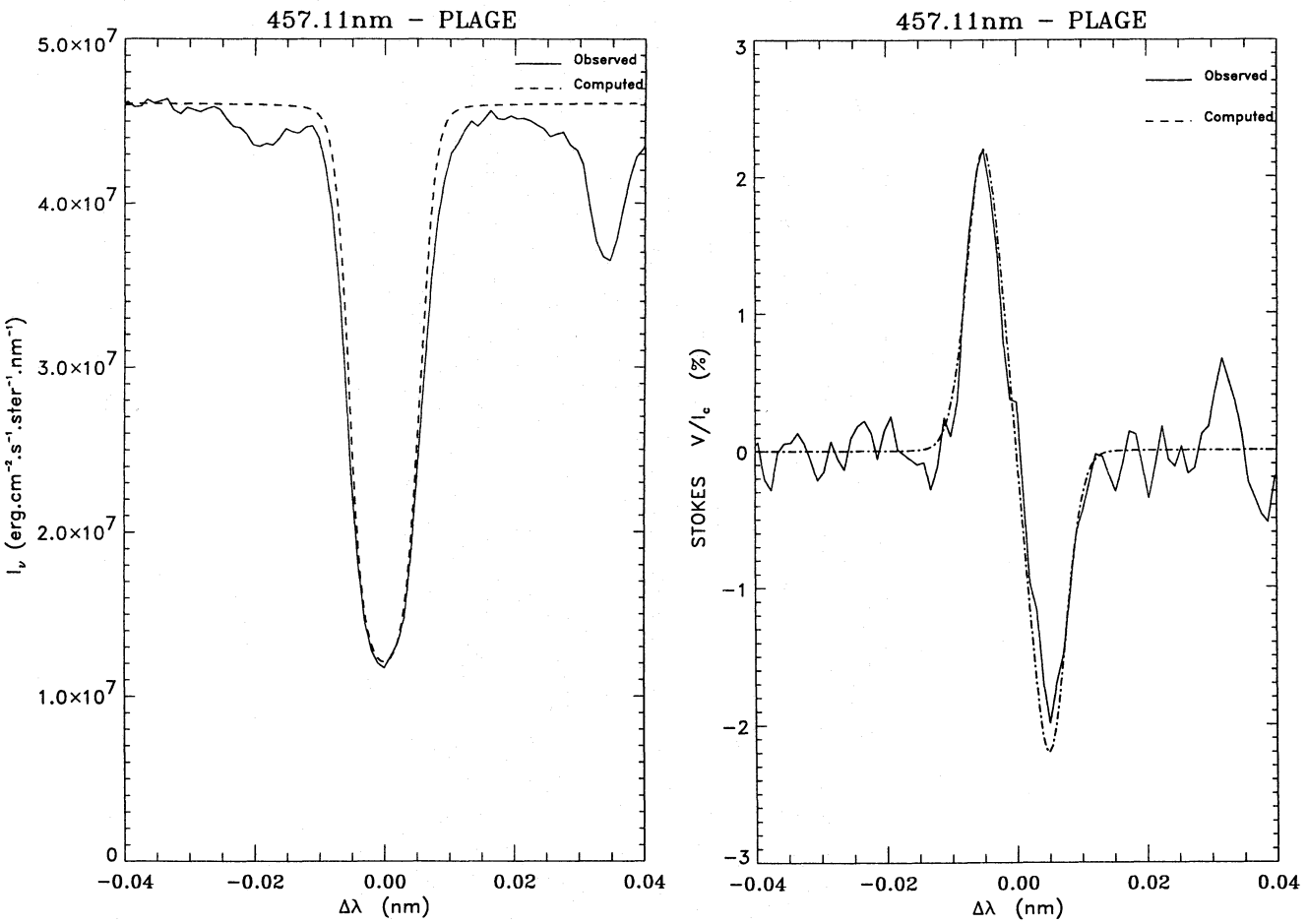

Fig. 15. Stokes I and V profiles of the λ457.1nm line computed for the PCHROM4 atmosphere in the flux tube and observed in an active region plage. A macroturbulent velocity of 1 km s^{-1} has been employed in addition to the microturbulence of 1.8 km s^{-1}

which is deeper than in the non-magnetic atmosphere, again in agreement with BS93. Our lines become insensitive to the temperature in higher layers (higher than $\log(\tau_{500}) \approx -4$). The V profiles are well reproduced by a microturbulence of 1.6 $\pm$ 0.1 km s^{-1} in the case of network magnetic element, and 1.8 $\pm$ 0.1 km s^{-1} in plage. In the quiet Sun, the observed b_2 line only requires a microturbulent velocity of approximately 1 km s^{-1} to be reproduced. The energy density in the line broadening motions in the upper photospheric layers of magnetic elements are thus a factor of 3 larger than in the quiet Sun. The λ457.1nm line, however, shows little difference in kinetic energy density between the three data sets. Thus, it is mainly in the higher layers that magnetic elements exhibit larger non-stationary motions than the quiet Sun. Although our models give satisfactory fits to Stokes V, they are not equally successful with Stokes I. This suggests that the upper photospheric layers of the non-magnetic atmosphere between magnetic elements differs from the average quiet Sun.

The main difference, besides the chromosphere, between the present models and earlier Stokes V based models of magnetic elements lies in the temperature drop in the mid-photosphere present in earlier models (e.g. Fig. 4), but absent or greatly reduced in the present model (Fig. 11). Since older models are all based on studies of Fe I and II lines, while the present models are based on a combination of C I lines (continuum-forming layers), Fe I and II (lower photosphere, chromospheric temperature rise), and Mg I (upper photosphere), we expect them to be more reliable than previous models. Purely iron-line based models in which the temperature within magnetic elements is not allowed to vary horizontally may well artificially give rise to such a temperature jump in the mid photosphere, since the thermophobe low excitation Fe I lines are formed at or above this level, where the temperature drops rapidly, while the thermophile Fe II lines are formed in the deeper, hotter layers (Holweger, private communication). A possible next step in the empirical modelling of the magnetic element thermal structure is to simultaneously use all available diagnostics to produce a consistent model.

Acknowledgements. We thank J.H.M.J. Bruls, H. Uitenbroek and G. Murphy for providing us with the codes and model atoms with which most of the calculations were carried out. H. Uitenbroek also kindly provided us with the Kitt Peak spectral atlas of White et al. (1972).

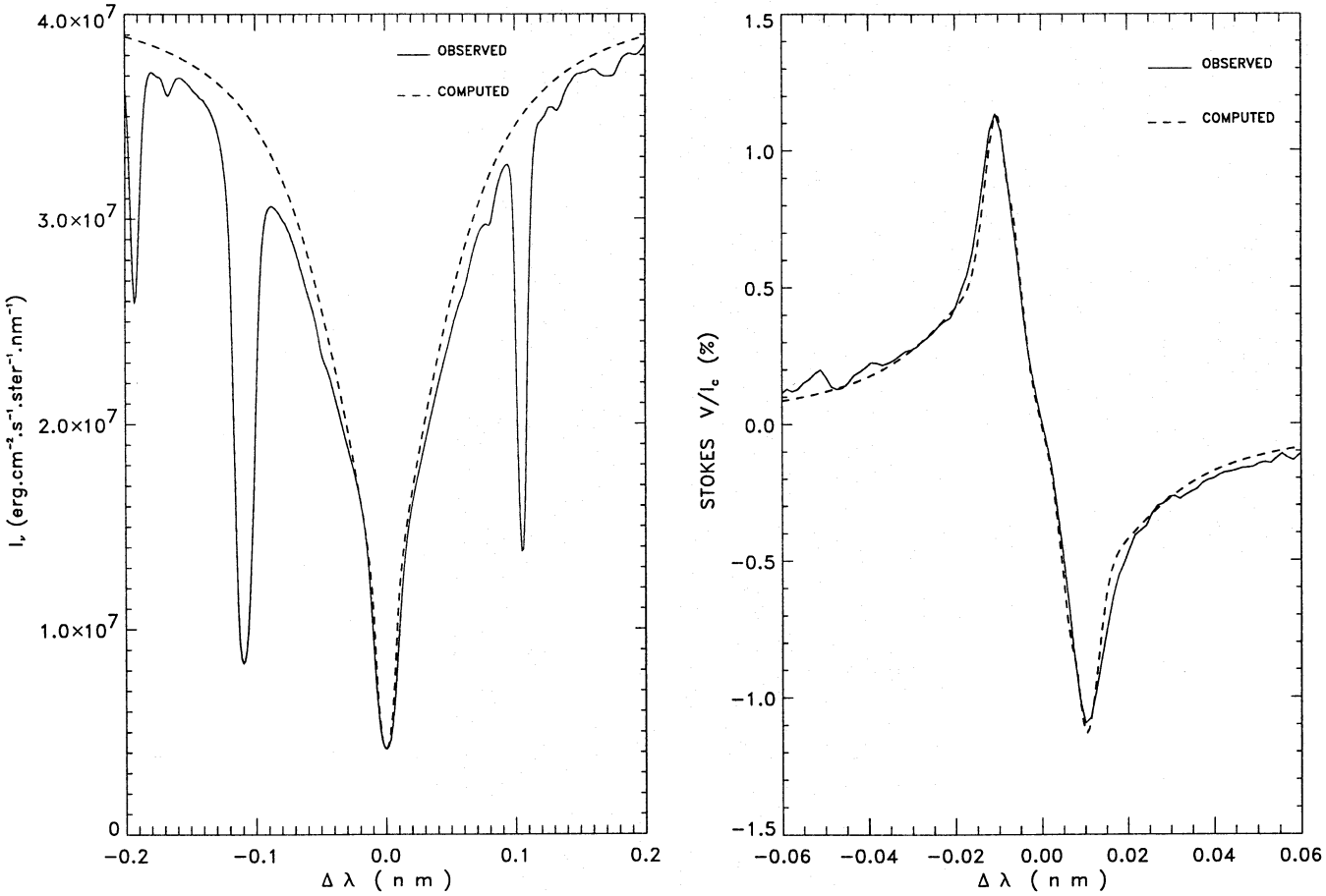

Fig. 16. The same as Fig. 16 for the λ517.3nm line (no macroturbulence was employed)

We are grateful to J.H.M.J. Bruls and H. Uitenbroek for clarifying discussions and for helping us to get started with MULTI.

One of the authors (C. Briand) has been supported by the french GDR "Magnétisme dans les étoiles de type solaire"

References

Allen, C.W., 1976, Astrophysical Quantities, Athlone Press, London
Auer, L.H., Heasley, J.N., House, L.L., 1977, ApJ, 216, 531
Ayres, T.R., 1981, ApJ, 244, 1064
Ayres, T.R., Testerman, L., 1981, ApJ, 245, 1124
Ayres, T.R., Testerman, L., Brault, J.W., 1986, ApJ, 304, 542
Bruls, J.H.M.J., Solanki, S.K., 1993, A&A, 273, 293
Carlsson, M., 1986, Uppsala Astronomical Observatory report 33
Carlsson, M., Rutten, R.J., Shchukina, N.G., 1992, A&A, 253, 576
Defouw, R.J., 1976, ApJ, 209, 266
Fontenla, J.M., Avrett, E.H., Loeser, R., 1993, ApJ, 406, 319
Gingerich, O., Noyes, R. W., Kalkofen, W., Cuny, Y., 1971, Solar Phys., 18, 347
Grossmann-Doerth, U., Schüssler, M., Solanki, S.K., 1988, A&A, 206, L37
Grossmann-Doerth, U., Knölker, M., Schüssler, M., Solanki, S.K., 1994, A&A, 285, 648
Hirayama, T., 1978, Publ. Astron. Soc. Japan, 30, 337
Hofsaess, D., 1979, Atomic Data and Nuclear Data Tables, 24, 285
Holweger, H., Müller, E.A., 1974, Solar Phys., 39, 19
Keller, C.U., Solanki, S.K., Steiner, O., Stenflo, J.O., 1990, A&A, 233, 583
Lemke, M., 1986, Diplomarbeit, University of Kiel
Lemke, M., Holweger, H., 1987, A&A, 173, 375
Lites, B.W., Skumanich, A., Rees, D.E., Murphy, G.A., Carlsson, M., 1987, ApJ, 318, 930
Lites, B.W., Skumanish, A., Rees, D.E., Murphy, G.A., 1988, ApJ, 330, 493
Lwin, N., McCartan, D.G., Lewis, E.L., 1977, ApJ, 213, 599
Maltby, P., Avrett, E.G., Carlsson, M., et al., 1986, ApJ, 306, 284
Martínez Pillet, V., García López, R.J., Del Toro Iniesta, J.C., 1990, ApJ, 361, L81
Mauas, P.J., Avrett, E.H., Loeser, R., 1988, ApJ, 330, 1008
Mendoza, C., Zeippen, C.J., 1987, A&A, 179, 339
Murphy, G.A., Rees, D.E., 1990, NCAR Technical Note - 348+IA
O'Neil, J.A., Smith, G., 1980, A&A, 81, 100
Pneuman, G.W., Solanki, S.K., Stenflo, J.O., 1986, A&A, 154, 231
Rees, D.E., 1969, Solar Phys., 10, 268
Rees, D.E., Murphy, G.A., Durrant, C.J., 1989, ApJ, 339, 1093
Scharmer, G.B., Carlsson, M., 1985, J. Comput. Phys., 59, 66
Schüssler, M., 1986, Small scale magnetic flux concentrations in the solar photosphere, W. Deinzer, M.K. Knölker, H. H. Voigt (Eds), Vandenhoeck and Ruprecht, Göttingen, p 103
Spruit, H.C., Roberts, B., 1983, Nature, 304, 401

Solanki, S.K., 1986, A&A, 168, 311
Solanki, S.K., 1987, PhD thesis, ETH-Zürich
Solanki, S.K., Brigljević, V., 1992, A&A, 262, L29
Solanki, S.K., Keller, C., Stenflo, J.O., 1987, A&A, 188, 183
Solanki, S.K., Livingston, W., Ayres, T., 1994, Science, 263, 64
Solanki, S.K., Roberts, B., 1992, M.N.R.A.S, 256, 13
Solanki, S.K., Steiner, O., 1990, 234, 519
Solanki, S.K., Steiner, O., Uitenbroek, H., 1991, A&A, 250, 220
Solanki, S. K., Stenflo, J. O., 1984, A&A, 140,185
Steiner, O., Pizzo, V.J., 1989, A&A, 211, 447
Stenflo, J.O, Harvey, J.W., Brault, J.W., Solanki, S.K., 1984, A&A, 131, 333
Uitenbroek, H., 1989, A&A, 216, 310
Uitenbroek, H., Noyes, R.W., Rabin, D., 1994, ApJ, 432, L67
Unsöld, A., 1955, Physik der Sternatmosphären, 2nd ed., Springer, Berlin
Walton, S.R., 1987, ApJ, 312, 909
White, O.R., Altrock, R.C., Brault, J.W., Slaughter, C.D., 1972, Solar Phys., 23, 18

This article was processed by the author using Springer-Verlag LaTeX A&A style file version 3.